

Using pattern recognition of epigenetic signals for supervised enhancer prediction

Anurag Sethi^{1,2}, Mengting Gu¹, Emrah Gumusgoz⁶, Landon Chan³, Koon-Kiu Yan^{1,2}, Kevin Yip⁴, Joel Rozowsky^{1,2}, Richard Sutton⁶, and Mark Gerstein¹

¹ Program in Computational Biology and Bioinformatics, Yale University, New Haven, Connecticut, United States of America ² Molecular Biophysics and Biochemistry, Yale University, New Haven, Connecticut, United States of America ³ School of Medicine, The Chinese University Hong Kong, China ⁴ Department of Computer Science, The Chinese University Hong Kong, China ⁵ Department of Computer Science, Yale University, New Haven, Connecticut, United States of America ⁶ Department of Internal Medicine, Section of Infectious Diseases, Yale University School of Medicine, New Haven, Connecticut, United States of America

Submitted to Proceedings of the National Academy of Sciences of the United States of America

Enhancers are important noncoding elements. Unfortunately, until recently, they were difficult to characterize experimentally, and only a few mammalian enhancers were validated, making it difficult to properly train statistical models for their identification. Instead, postulated patterns of genomic features were used heuristically for identification. Recently, a large number of massively parallel assays for characterizing enhancers have been developed. Here, we use them to create shape-matching filters based on enhancer-associated metaprofiles in epigenetic features. We then combine different features with simple, linear models and predict enhancers in a supervised fashion. By cross-validating and testing our models, we show that they can be transferred without reparameterization between cell lines and even between organisms. Finally, we predict enhancers in cell lines with many transcription-factor binding sites and validate these enhancers experimentally. In turn, this highlights distinct differences between the type of binding at enhancers and promoters, enabling the construction of a secondary model discriminating between these two.

Epigenetics | Transcription factors | Enhancer prediction | Matched filter | Machine Learning

Introduction

Enhancers are gene regulatory elements that activate expression of target genes from a distance [1]. Enhancers are turned on in a space and time-dependent manner contributing to the formation of a large assortment of cell-types with different morphologies and functions even though each cell in an organism contains a nearly identical genome [2-4]. Moreover, changes in the sequences of regulatory elements are thought to play a significant role in the evolution of species [5-9]. Understanding enhancer function and evolution is currently an area of great interest because variants within distal regulatory elements are also associated with various traits and diseases during genome-wide association studies [10-12]. However, the vast majority of enhancers and their spatiotemporal activities remain unknown because it is not easy to predict their activity based on DNA sequence or chromatin state [13, 14].

Traditionally, the regulatory activity of enhancers and promoters were experimentally validated in a non-native context using low throughput heterologous reporter constructs leading to a small number of validated enhancers that function in the same mammalian cell-type [15, 16]. In addition to the small numbers, the validated enhancers were typically selected based on conserved noncoding regions [17] with particular patterns of chromatin [18], transcription-factor binding, [19] or noncoding transcription [20]. The small number and biases within the validated enhancers make them inappropriate for parameterizing tissue-specific enhancer prediction models [16]. As a result, most theoretical methods to predict enhancers could not optimally parameterize their models using a gold standard set of functional elements. Instead, most of these models were parameterized based

on certain heuristic features associated with enhancers, which were then utilized to predict enhancers [19, 21-30]. For example, two of the widest used methods for predicting enhancers were based on the fact that these elements are expected to contain a cluster of transcription factor binding sites [24] and their activity is often correlated with an enrichment of certain post-translational modifications on histone proteins [27, 30]. These predictions were not rigorously assessed as very few putative enhancers could be validated experimentally and it remains challenging to assess the performance of different methods for enhancer prediction.

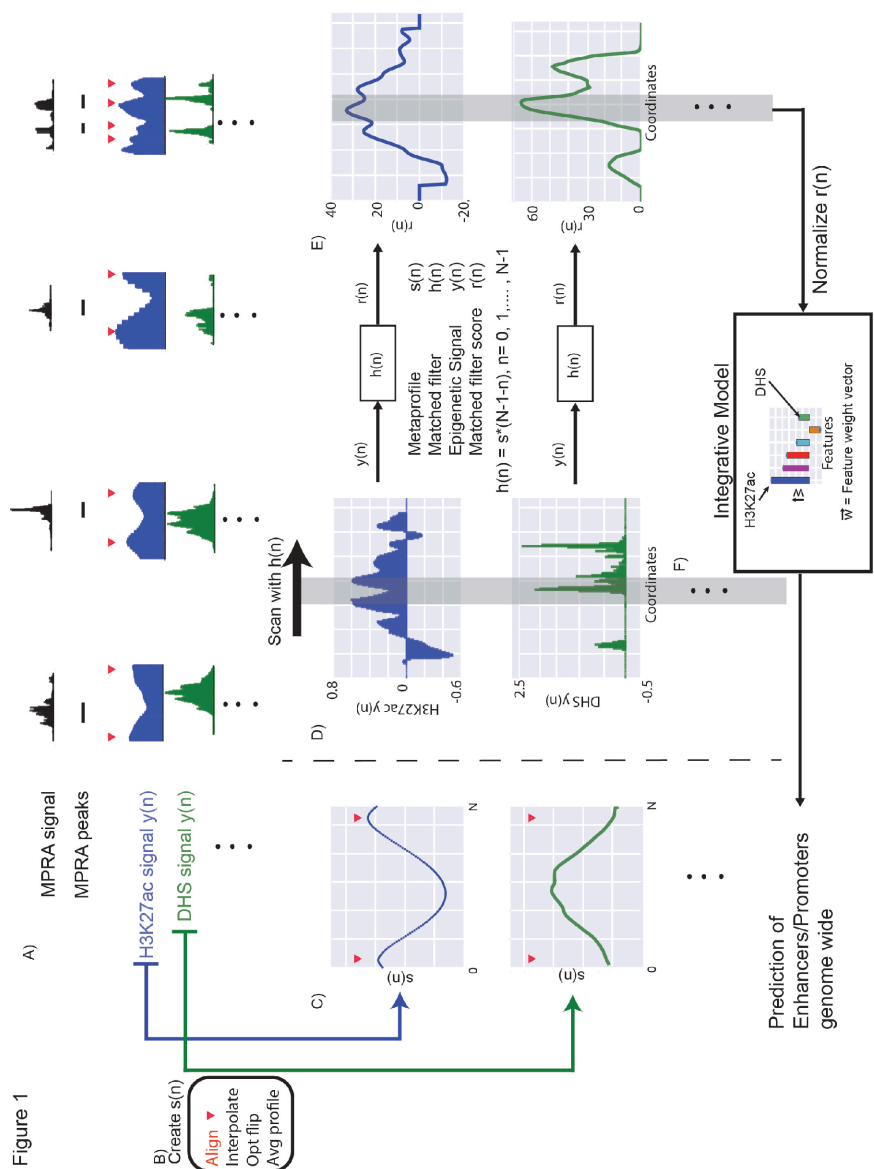
In recent times, due to the advent of next generation sequencing, a number of transfection and transduction-based assays were developed to experimentally test the regulatory activity of thousands of regions simultaneously in a massively parallel fashion [31-37]. In these experiments, several plasmids that each contains a single core promoter upstream of a luciferase or GFP gene are transfected or transduced into cells. These plasmids are used to test the regulatory activity of different regions by placing one region near the core promoter in each plasmid as differences in the gene's expression occur due to the differences in the activity of the tested region. STARR-seq was one such massively parallel reporter assay (MPRA) that was used to test the regulatory activity of the fly genome in several cell-types [31, 38] and was used to identify thousands of cell-type specific enhancers and promoters. MPRA has confirmed that active enhancers and promoters tend to be depleted of histone proteins and contain accessible DNA on which various transcription factors and co-factors bind [39, 40]. These regulatory regions also tend to be flanked by nucleosomes that contain histone proteins with certain

Significance

Enhancers are important regulatory elements in the genome. The distance between the enhancer and its regulating genes varies between several kilobytes to megabytes, making it hard to annotate enhancer regions both experimentally and computationally. Here we demonstrate that by integrating epigenetic features with supervised machine learning models, we can achieve high accuracy of enhancer prediction. The match filter tool providing a general framework to identify enhancers across cell lines.

Reserved for Publication Footnotes

137
138
139
140
141
142
143
144
145
146
147
148
149
150
151
152
153
154
155
156
157
158
159
160
161
162
163
164
165
166
167
168
169
170
171
172
173
174
175
176
177
178
179
180
181
182
183
184
185
186
187
188
189
190
191
192
193
194
195
196
197
198
199
200
201
202
203
204



PDF

Fig. 1. Creation of metaprofile. A) We identified the “double peak” pattern in the H3K27ac signal close to STARR-seq peaks. The red triangles denote the position of the two maxima in the double peak. B) We aggregated the H3K27ac signal around these regions after aligning the flanking maxima, using interpolation and smoothing on the H3K27ac signal, and averaged the signal across different MPRA peaks to create the metaprofile in C). The exact same operations can be performed on other histone signals and DHS to create metaprofiles in other dependent epigenetic signals. D) Matched filters can be used to scan the histone and/or DHS datasets to identify the occurrence of the corresponding pattern in the genome. E) The matched filter scores are high in regions where the profile occurs (grey region shows an example) and it is low when only noise is present in the data. The individual matched filter scores from different epigenetic datasets can be combined using integrative model in F) to predict active promoters and enhancers in a genome wide fashion.

205
206
207
208
209
210
211
212
213
214
215
216
217
218
219
220
221
222
223
224
225
226
227
228
229
230
231
232
233
234
235
236
237
238
239
240
241
242
243
244
245
246
247
248
249
250
251
252
253
254
255
256
257
258
259
260
261
262
263
264
265
266
267
268
269
270
271
272

characteristic post-translational modifications. These attributes lead to an enriched peak-trough-peak (“double peak”) signal in different ChIP-Seq experiments for various histone modifications such as acetylation on H3K27 and methylations on H3K4. The troughs in the double peak ChIP-seq signal represent the accessible DNA that leads to a peak in the DNase-I hypersensitivity (DHS) at the enhancer [41]. However, the optimal method to combine information from multiple epigenetic marks to make cell-type specific regulatory predictions remains unknown. For the first time, using data from several MPRA, we have the ability to properly train our models based on a large number of experimentally validated enhancers and test the performance of different models for enhancer prediction using cross validation.

We developed a new supervised machine-learning method that was trained and tested on large number of experimentally active regulatory regions identified in MPRA to accurately predict active enhancers and promoters in a cell-type specific manner. Unlike previous prediction methods that focused on the enrichment (or signal) of different epigenetic datasets, we developed a method to also take into account the enhancer-associated pattern within different epigenetic signals. As the epigenetic signal

around each enhancer is noisy, we aggregated the signal around thousands of enhancers identified using MPRA to increase the signal-to-noise ratio and identified the shape associated with active regulatory regions. The epigenetic signal shapes associated with promoters and enhancers are conserved across millions of years of evolution and these models can be used to predict enhancers and promoters in different cell-types and tissues and across diverse eukaryotic species. We further created simple to use transferrable statistical models with six parameters that can be used to predict enhancers and promoters in several eukaryotic species including fly, mouse, and human. We applied these models to predict active enhancers and promoters in the H1-human embryonic stem cell (H1-hESC), a highly studied human cell-line in the ENCODE datasets. These analyses show that the pattern of transcription factor (TF) binding and co-binding varies between enhancers and promoters. The pattern of TF and co-TF binding at active enhancers is much more heterogeneous than the corresponding patterns on promoters. The pattern of TF binding can be used to distinguish enhancers from promoters with high accuracy. Thus, our methods provide a framework that utilizes different epigenetic genomics datasets to predict active regulatory

273
274
275
276
277
278
279
280
281
282
283
284
285
286
287
288
289
290
291
292
293
294
295
296
297
298
299
300
301
302
303
304
305
306
307
308
309
310
311
312
313
314
315
316
317
318
319
320
321
322
323
324
325
326
327
328
329
330
331
332
333
334
335
336
337
338
339
340

Figure 2

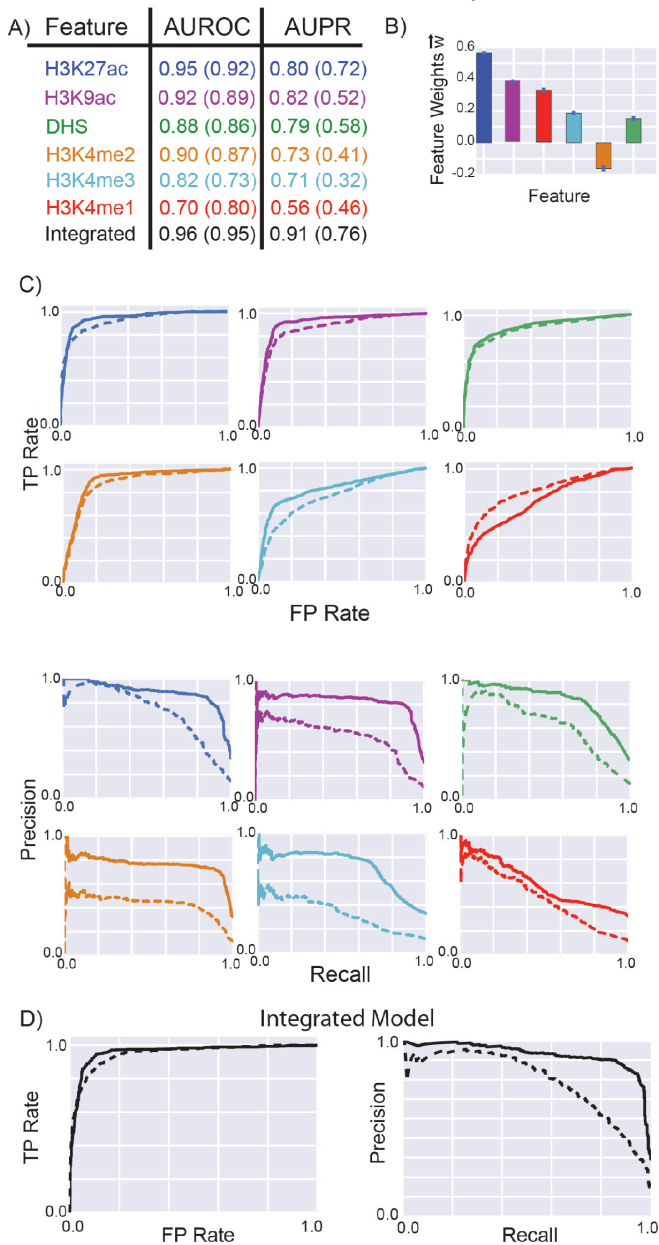


Fig. 2. Performance of matched filters and integrated models for predicting MPRA peaks. The performance of the matched filters of different epigenetic marks and the integrated model for predicting all STARR-seq peaks is compared here using 10-fold cross validation. A) The area under the receiver-operating characteristic (AUROC) and the precision-recall (AUPR) curves are used to measure the accuracy of different matched filters and the integrated model. B) The weights of the different features in the integrated model are shown and these weights may be used as a proxy for the importance of each feature in the integrated model. C) The individual ROC and PR curves for each matched filter and the integrated model are shown. The performance of these features and the integrated model for predicting the STARR-seq peaks using multiple core promoters and single core promoter are compared. The numbers within the parentheses in A) refer to the AUROC and AUPR for predicting the peaks using a single STARR-seq core promoter while the numbers outside the parentheses refers to the performance of the model for predicting peaks from multiple core promoters.

regions in a cell-type specific manner and then utilizes further

Figure 3

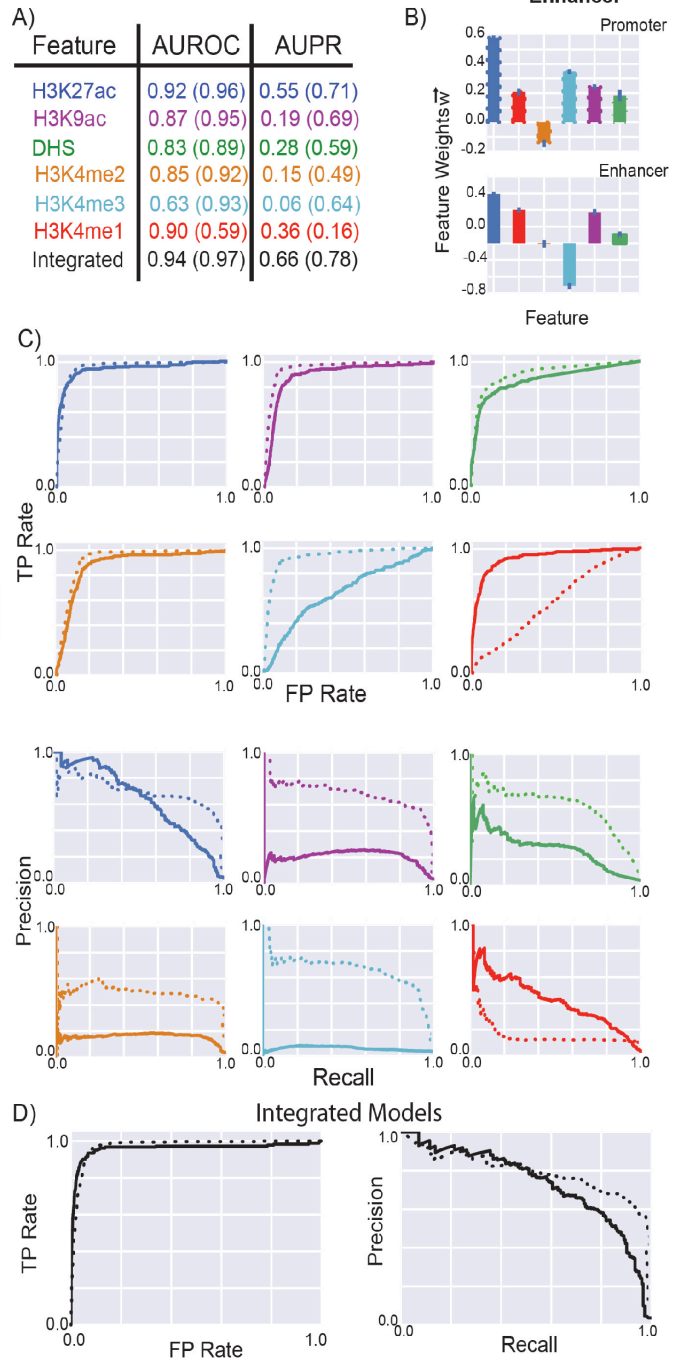


Fig. 3. Performance of matched filters and integrated models for predicting promoters and enhancers. The performance of the matched filters of different epigenetic marks and the integrated model for predicting active promoters and enhancers are compared here using 10-fold cross validation. A) The numbers within parentheses refer to the AUROC and AUPR for predicting promoters while the numbers outside parentheses refer the performance of the models for predicting enhancers. B) The weights of the different features in the integrated models for promoter and enhancer prediction are shown. C) The individual ROC and PR curves for each matched filter and the integrated model are shown. The performance of these features and the integrated model for predicting the active promoters and enhancers using multiple core promoters are compared.

functional genomics datasets to identify key TFs associated with active regulatory regions within these cell-types.

341
342
343
344
345
346
347
348
349
350
351
352
353
354
355
356
357
358
359
360
361
362
363
364
365
366
367
368
369
370
371
372
373
374
375
376
377
378
379
380
381
382
383
384
385
386
387
388
389
390
391
392
393
394
395
396
397
398
399
400
401
402
403
404
405
406
407
408

Figure 4

Fly-based models on mouse

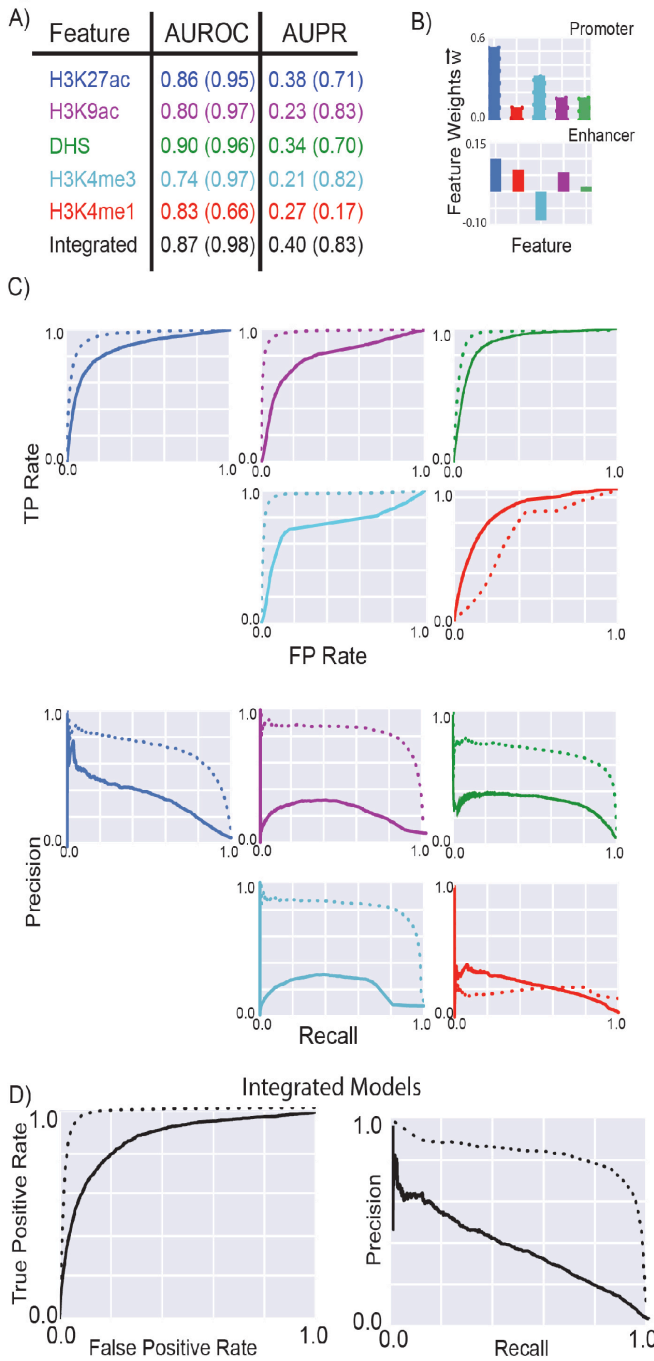


Fig. 4. Conservation of epigenetic features. The performance of the fly-based matched filters and the integrated model for predicting active promoters and enhancers in mouse embryonic stem cells identified using FIREWACH. A Similar to Figure 3, the numbers within parentheses refer to the AUROC and AUPR for predicting promoters while the numbers outside parentheses refer the performance of the models for predicting enhancers. B) The weights of the different features in the integrated models for promoter and enhancer prediction are shown. C) The individual ROC and PR curves for each matched filter and the integrated model are shown. The performance of these features and the integrated model for predicting the active promoters and enhancers identified using FIREWACH are shown.

Results

Aggregation of epigenetic signal to create metaprofile:

We developed a framework to predict activating regulatory elements utilizing the epigenetic signal patterns associated with experimentally validated promoters and enhancers [31]. We aggregated the signal of histone modifications on MPRA peaks to remove noise in the signal and created a metaprofile of the double peak signals of histone modifications flanking enhancers and promoters. MPRA peaks typically consist of a mixture of enhancers and promoters, and at this stage, we do not differentiate between the two sets of regulatory elements. These metaprofiles were then utilized in a pattern recognition algorithm for predicting active promoters and enhancers in a cell-type specific manner.

These metaprofiles were initially created using the histone modification H3K27ac at active STARR-seq peaks (see Figure 1 and Methods) identified in the S2 cell-line of fly. Approximately 70% of the active STARR-seq peaks contain an easily identifiable double peak pattern even though there is a lot of variability in the distance between the two maxima of the double peak in the ChIP-chip signal (Figure S1). Even though the minimum tends to occur in the center of these two maxima on average, the distance between the two maxima in the double peaks can vary between 300 and 1100 base pairs. During aggregation, we aligned the two maxima in the H3K27ac signal across different STARR-seq peaks, followed by interpolation and smoothening the signal before calculating the average metaprofile. In addition, an optional flipping step was performed to maintain the asymmetry in the underlying H3K27ac double peak because it may be associated with the directionality of transcription [42]. For the first time, we also calculated the dependent metaprofiles for thirty other histone marks and DHS signal by applying the same set of transformations to these datasets. The metaprofile for the histone marks associated with active regulatory regions were also double peak signals and the maxima across different histone modification signals tended to align with each other on average (Figure S2). This indicates that a large number of histone modifications tend to simultaneously co-occur on the nucleosomes flanking an active enhancer or promoter. In contrast, as expected, the DHS signal displayed a single peak at the center of the H3K27ac double peak (Figure 1). In addition, repressive marks such as H3K27me3 were depleted in these regions and the metaprofile for these regions did not contain a double peak signal (Figure S2).

Occurrence of metaprofile is predictive of regulatory activity:

We evaluated whether these metaprofiles can be utilized to predict active promoters and enhancers using matched filters, a well-established algorithm in template recognition. A matched filter is the optimal pattern recognition algorithm that uses a shape-matching filter to recognize the occurrence of a template in the presence of stochastic noise [43]. We evaluated whether the occurrence of the epigenetic metaprofiles identified for the histone marks and DHS can be used to predict active enhancers and promoters using receiver operating characteristic (ROC) and precision-recall (PR) curves. The PR curves are particularly useful to assess the performance of classifiers in skewed or imbalanced data sets in which one of the classes is observed much more frequently as compared to the other. On these imbalanced data sets, PR curves are useful alternative to ROC curves as the precision is directly related to the false detection ratio at different thresholds. The PR curve highlights differences in performance of different models even when their ROC curves remain comparable [44]. The matched filter score is higher in genomic regions where the template pattern occurs in the corresponding signal track while it is low when only noise is present in the signal (Figure 1). Due to the aforementioned variability in the double peak pattern, the H3K27ac signal track is scanned with multiple matched filters with templates that vary in width between the two maxima in the double peak and the highest matched filter score with these matched filters is used to rate the regulatory potential of this region (see Methods). The dependent profiles are then used on the

Figure 5

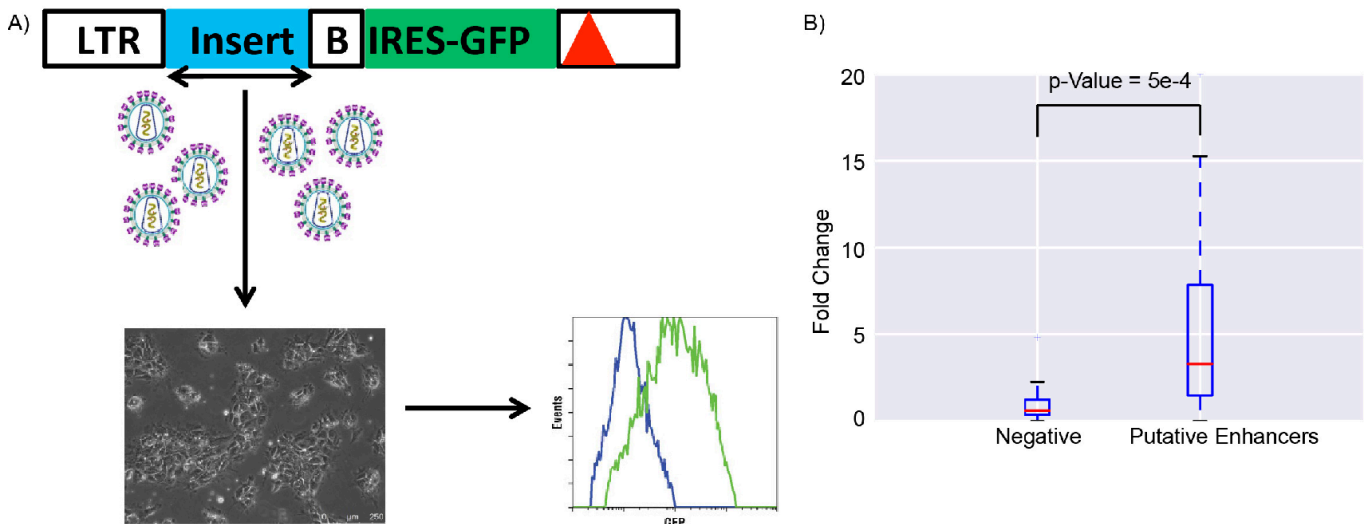


Fig. 5. Enhancer Validation Experiments. A) A schematic of the enhancer validation scheme is shown. At top is third generation HIV-based self-inactivating vector (deletion in 3' LTR indicated by red triangle), with PCR-amplified test DNA (blue, two-headed arrow indicates fragment was cloned in both orientations), inserted just 5' of a basal (B) Oct4 promoter driving IRES-eGFP (green). Vector supernatant was prepared by plasmid co-transfection of 293T cells and used to transduce cellular targets and analyzed by flow cytometry a few days later. B) The fold change of gene expression of eGFP is compared between negative elements and putative enhancers chosen for experiments. The p-Value of the difference in activity is measured using a Wilcoxon signed-rank test.

same region with the matched filter to score the corresponding genomic tracks.

We used 10-fold cross validation to assess the performance of matched filters for individual histone marks to predict active STARR-seq peaks. In Figure 2, we observe that the H3K27ac matched filter is the single most accurate feature for predicting active regulatory regions (AUROC=0.92, AUPR=0.72) identified using STARR-seq. This is consistent with the literature as H3K27ac enriched peaks are often used to predict active promoters and enhancers [23, 45, 46]. In general, several histone acetylation (H3K27ac, H3K9ac, H4K12ac, H2BK5ac, H4K8ac, H4K5ac, H3K18ac) marks as well as the H1, H3K4me2, and DHS matched filters are the most accurate marks (see Figure 2 and Table S1) because the matched filter scores for these regions on these marks are higher for STARR-seq peaks (Figure S3). The degree to which the matched filter scores for promoters and enhancers are higher than the matched filter scores for the rest of the genome is a measure of the signal to noise ratio for regulatory region prediction in the corresponding feature's genomic track and the larger the separation between positives and negatives, the greater the accuracy of the corresponding matched filter for predicting active regulatory regions. Interestingly, the distribution of matched filter scores for STARR-seq peaks are unimodal for each histone mark except for H3K4me1, H3K4me3, and H2Av, which are bimodal (Figure S3). We also show that the matched filter scores are more accurate for predicting active STARR-seq peaks than enrichment of signal alone as they outperform the histone peaks on ROC and PR curves (Figure S4).

While a single STARR-seq experiment identifies thousands of active regulatory regions, these regions display core-promoter specificity and different sets of enhancers are identified when different core promoters are used in the same cell-type [47-51]. As we wanted to create a framework to predict all the enhancers and promoters active in a particular cell-type, we combined the peaks identified from multiple STARR-seq experiments in the S2 cell-type and reassessed the performance of the matched filters at predicting these regulatory regions. Merging the STARR-seq peaks from multiple core promoters in the S2 cell-type leads to

higher AUROC and AUPR for the matched filters from most histone marks (Figure 2).

Machine learning can combine matched filter scores from different epigenetic features:

We combined the normalized matched filter scores (see Methods) from six different epigenetic marks (H3K27ac, H3K4me1, H3K4me2, H3K4me3, H3K9ac, and DHS) associated with active regulatory regions by the Roadmap Epigenomics Mapping [52] and the ENCODE [53] Consortia using a linear SVM [54] and the integrated model achieved a higher accuracy than the individual matched filter scores (Figure 2). We also assessed the performance of other statistical approaches for combining the features (including non-linear models) in Figure S6 and all these models performed similarly. By using only six features, we ensure that our model is capable of being applied to many cell-lines and tissues on which the relevant experiments have been performed. These models are trained to learn the patterns in the matched filter scores for different epigenetic marks within experimentally verified regulatory regions and we chose these marks as we wanted to assess the applicability of these machine learning models to predict active enhancers and promoters across different cell-types and species. As expected, the integrated models outperformed the individual matched filter scores, as they are able to leverage information from multiple epigenetic marks. In addition, the six-parameter integrated model displayed higher accuracy after combining the peaks identified using different core promoters. In the integrated model, the normalized matched filter score for each epigenetic feature in a particular region is scaled by its optimized weight and added together to form the discriminant function. The sign of the discriminant function is then used to predict whether the region is regulatory. The features with large positive and negative weights are predicted to be important for discriminating regulatory regions from non-regulatory regions in such models. They can also be used to measure the amount of non-redundant information added by each feature in the integrated model. According to the model, the acetylations (H3K27ac and H3K9ac) are the most important feature for

Figure 6

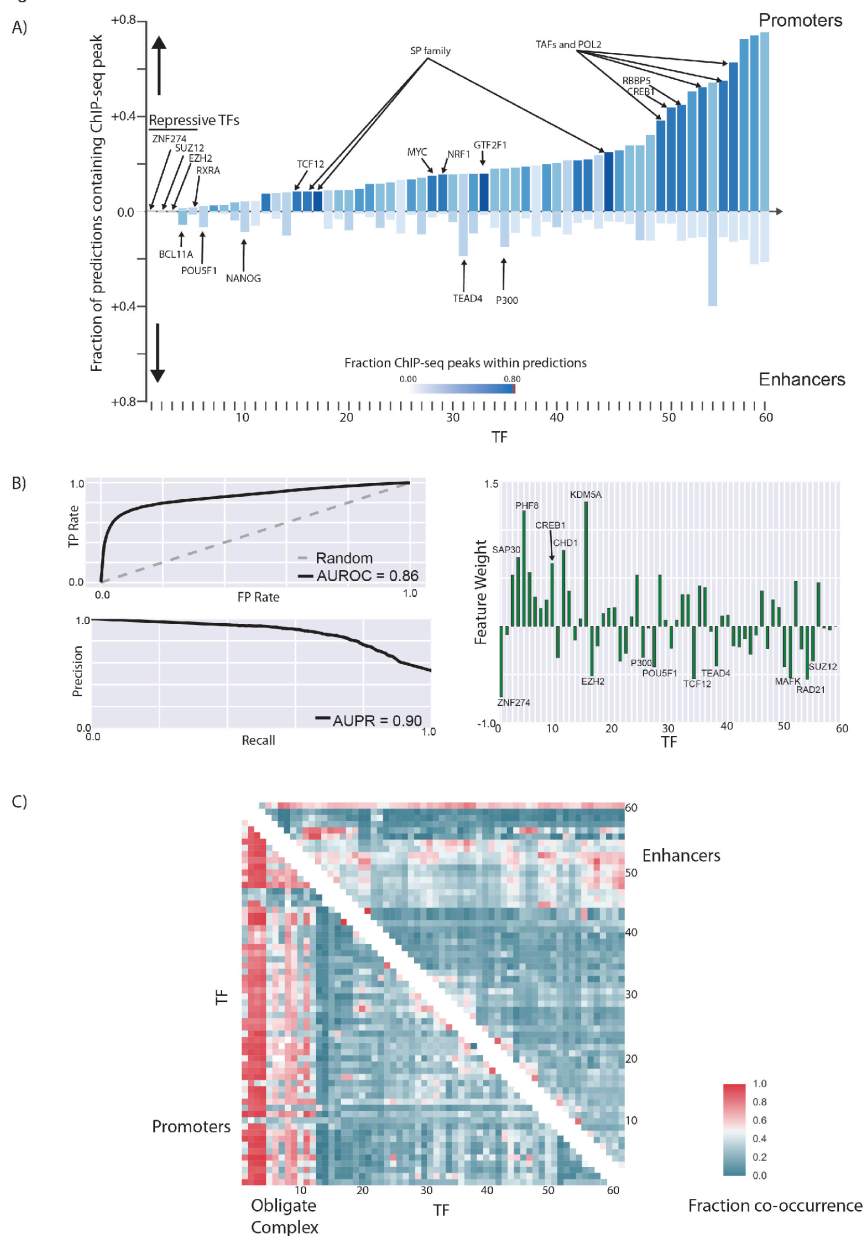


Fig. 6. Differences in TF binding patterns at enhancers and promoters. A) The fraction of predicted promoters and enhancers that overlap with ENCODE ChIP-seq peaks for different TFs in H1-hESC are shown. The names of all TFs in the figure can be viewed in Figure S19. B) The AUROC and AUPR for a logistic regression model created using the pattern of TF binding at each regulatory region to distinguish enhancers from promoters are shown. The weight of each feature in the logistic regression model can be used to identify the most important TFs that distinguish enhancers from promoters. C) The patterns of TF co-binding at active promoters and enhancers are shown. The names of all the TFs in this graph can be viewed in Figure S20.

predicting active regulatory regions from inactive regions. While the DHS matched filter performed well as an individual feature (AUPR in Figure 2), the information in DHS is redundant with the information in the histone marks as indicated by the fact that it has the lowest weight among the six features in the integrated model. We compared several other machine learning algorithms including nonlinear SVM (results not shown) to combine the machine learning models and found that they all displayed nearly similar accuracy and similar features were more important across these different models (Figure S5).

To assess the information contained in other epigenetic marks, we combined the matched filters from all 30 measured histone marks along with the DHS matched filter in separate statistical models (Figure S6) and these model displayed higher accuracy (AUROC=0.97, AUPR=0.93 for SVM model with multiple core promoters) than the 6 feature model presented in Figure 2. The feature weights in this model indicated that H3K27ac

contains the most information regarding the activity of regulatory regions. However, we found that a few other acetylations such as H2BK5ac, H4ac, and H4K12ac contain additional non-redundant information regarding the activity of these regulatory regions and might improve the accuracy of promoter and enhancer prediction from machine learning models (Figure S6).

Distinct epigenetic signals associated with promoters and enhancers:

We proceeded to create individual metaprofiles and machine learning models for the two classes of regulatory activators – promoters (or proximal) and enhancers (or distal). We divided all the active STARR-seq peaks into promoters or enhancers based on their distance to the closest transcription start site (TSS) to delineate their likely function in the native context. Due to the conservative distance metric used in this study (1kb upstream and downstream of TSS in fly), the enhancers are regulatory elements that are not close to any known TSS even though a few of the

817 promoters may actually function as enhancers. We then created
818 metaprofiles of the different epigenetic marks on the promoters
819 and enhancers and assessed the performance of the matched
820 filters for predicting active regulatory regions within each category (Figure 3). The highest matched filter scores are typically
821 observed on promoters and the matched filters for each of the six
822 features tended to perform better for promoter prediction. The
823 H3K27ac matched filter continues to outperform other epigenetic
824 marks for predicting active promoters and enhancers (Figure
825 3). In addition, the DHS, H3K9ac, and H3K4me2 matched
826 filters also performed reasonably for promoter and enhancer
827 prediction. Similar to previous studies [55, 56], we observed that the
828 H3K4me1 metaprofile performs better for predicting enhancers
829 while it is close to random for predicting promoters. In contrast,
830 the H3K4me3 metaprofile can be utilized to predict promoters
831 and not enhancers. The histogram for matched filter scores show
832 that H3K4me1 matched filter score is higher near enhancers
833 while the H3K4me3 matched filter score tends to be higher near
834 promoters (Figure S7). The mixture of these two populations lead
835 to bimodal distributions for H3K4me1 and H3K4me3 matched
836 filter scores when calculated over all regulatory regions (Figure
837 S3).

839 We created two different integrated models to learn the combination of features associated with promoters and enhancers.
840 These integrated models outperformed the individual matched
841 filters at predicting active enhancers and promoters (Figures
842 3 and S8). In addition, the weights of the individual features
843 identified the difference in roles of the H3K4me1 and H3K4me3
844 matched filter scores at discriminating active promoters and
845 enhancers from inactive regions in the genome. The promoter-based
846 (enhancer-based) model performed much more poorly at
847 predicting enhancers (promoters) indicating the unique properties
848 of these regions (Figures S10 and S11). We also created two
849 integrated models utilizing matched filter scores for all thirty
850 histone marks as features for predicting enhancers and promoters.
851 The additional histone marks provided independent information
852 regarding the activity of promoters and enhancers as these features
853 increased the accuracy of these models (Figure S9). The weights
854 of different features indicate that H2BK5ac again displays the
855 most independent information for accurately predicting active
856 enhancers and promoters (Figures S9). We observe similar trends
857 and accuracy with several different machine learning models
858 (Figures S8 and S9).

860 **The epigenetic underpinnings of active regulatory regions are** 861 **highly conserved in evolution:**

862 In order to assess the transferability of these metaprofiles and machine learning models for predicting regulatory regions
863 in other tissues and cell-types, we assessed the accuracy of these
864 models for predicting regulatory elements identified using the
865 transduction-based FIREWACH assay in mouse embryonic stem
866 cells (mESC) [36]. The metaprofiles for individual histone marks
867 learned using active promoters and enhancers identified with the
868 STARR-seq assay in the S2 cell-line were used with matched
869 filters to predict the regulatory activity of different regions in
870 mESC based on the epigenetic signals in mESC (Figure 4). The
871 matched filters for individual histone marks displayed similar
872 accuracy for predicting enhancers and promoters in mESC as
873 in the original S2 cell-line. In addition, the 6-parameter SVM
874 models learned using STARR-seq data in S2 cell-line were also
875 highly accurate at predicting active enhancers and promoters in
876 mouse (Figure 4).

877 This indicates that the epigenetic profiles associated with
878 active enhancers and promoters are conserved over 600 million
879 years of evolution underscoring the importance of such epigenetic
880 modifications in maintaining the regulatory role of enhancers
881 and promoters across different cell-types and species. As these
882 regulatory regions were identified using a single core promoter in

885 FIREWACH, the performance of the different models in Figure 4
886 is probably underestimated. The accuracy of these models enables
887 us to use the metaprofiles and statistical models learned using
888 STARR-seq data in fly to predict enhancers in different cell-lines
889 and eukaryotic species. Consistent with this, the metaprofile and
890 machine learning models learned using STARR-seq experiment
891 in BG3 cell-line (fly) can be utilized to predict active promoters
892 and enhancers in the S2 cell-line (Figure S12).

893 **Validation of Enhancer Prediction Models**

894 The ENCODE consortium has ChIP-Seq data for 60 transcription related factors in H1-hESC cell line, including a few
895 chromatin remodelers and histone modification enzymes. Collectively we call all these transcription related factors "TF"s for
896 simplicity. We utilized the 6 parameter integrated model to predict active enhancers and promoters in the hESC cell-line based on
897 the epigenetic datasets measured by the ENCODE consortium. This provides us with a system to validate our enhancer prediction
898 model as well as to study the patterns of TF binding within enhancers and promoters. Using these models, we predicted 43463
899 active regulatory regions, of which 22828 (52.5%) are within 2kb of the TSS and are labeled as promoters. A large proportion of
900 the predicted enhancers are found in the introns (30.41%) and intergenic regions (13.93%) (Figure S13). The predicted promoters
901 and enhancers are significantly closer to active genes than might be expected randomly (Figure S14). By comparing the matched
902 filter predicted enhancers and promoters with chromatin states predicted by chromHMM [30] and SegWay [27], we observe that
903 a majority of the predicted enhancers and promoters are also predicted to be enhancers and promoters by chromHMM and
904 SegWay respectively (Figures S15 to S18).

905 A third generation, self-inactivating HIV-1 based vector system in which the eGFP reporter was driven by the DNA element
906 of interest was used to validate putative enhancers after stable transduction of various cell lines, including H1 hESC (Figure 5).
907 The predicted enhancers, ranging from 650 to 2500 bp, were PCR amplified from human genomic DNA and inserted just upstream
908 of a basal Oct-4 promoter of 142 bp (a housekeeping promoter is used so that the activity of the putative enhancers should be
909 similar across different cell lines). VSV G-pseudotyped vector supernatants from each were prepared by co-transfection of 293T
910 cells, and these were used to transduce the various cell lines, with empty vector and FG12 vector serving as negative and positive
911 controls, respectively. Putative enhancer activity was assessed by flow cytometric readout of eGFP expression 48-72 h post-
912 transduction, normalized to the negative control.

913 A total of 25 predicted intergenic enhancers were randomly selected for validation (Supplementary Table S3). These predictions
914 were chosen randomly to ensure that these truly represented the whole spectrum of predicted enhancers and not just the top
915 tier of predicted enhancers. Of these 25 putative enhancers, 23 were successfully amplified and cloned into the HIV vector. To
916 measure the distribution of gene expression in the absence of enhancer, we also amplified and cloned 25 non-repetitive elements
917 with similar length distribution that were predicted to be inactive using the same HIV vector. All positive and negative
918 DNA elements were transduced and tested for activity in both forward and reverse strand orientations since enhancers are thought
919 to function in an orientation-independent manner. Functional testing was performed in HOS, TZMBL, and A549 cell lines in
920 addition to H1-hESCs.

921 Insertion of twelve of the 23 putative enhancers into the HIV vector resulted in a significant increase in eGFP expression (P-
922 value < 0.05 over distribution of gene expression for negative elements) in the H1-hESCs (Supplementary Table S3). While most
923 of the positive enhancers displayed a significant increase in gene expression irrespective of their orientation during orientation,
924 a few elements showed significantly higher levels of gene expression

953 in one of the orientations (Supplementary Table S4). In contrast,
954 the negatives displayed much lower levels of gene expression
955 typically (Figure 5 and Supplementary Figure S19). In addition,
956 most of these elements increased gene expression of GFP in the
957 four different cell lines even though some of the elements were
958 preferentially active in one of the cell lines. Overall, 16 of the
959 23 tested predictions displayed statistically significant increase in
960 gene expression of the reporter gene in at least one of the cell lines
961 (Supplementary Table S3 and Supplementary Figure S19). Given
962 the promoter specificity of enhancers in such assays, we would
963 anticipate that some of the elements that could not be validated
964 in this particular vector would function as enhancers in a more
965 natural biological context.

966 **Different Transcription Factors bind to enhancers and pro-** 967 **motors**

968 We further studied the differences in TF binding at promoters
969 and enhancers (Figure 6 and Figure S20). Most promoters and
970 enhancers contain multiple TF-binding sites. However, the TF-
971 binding of enhancers is more heterogeneous than promoters: in
972 particular, more than 70% of the promoters bind to the same set
973 of 2-3 sequence-specific TFs, which is not observed for enhancers.
974 The majority of the promoters also contain peaks for several
975 TATA-associated factors (TAF1, TAF7, and TBP). Overall, the
976 high heterogeneity associated with enhancer TF-binding is con-
977 sistent with the absence of a sequence code (or grammar) which
978 can be utilized to easily identify active enhancers on a genome-
979 wide fashion.

980 In Figure 6, we show that the patterns of TF binding within
981 regulatory regions can be utilized in a logistic regression model to
982 distinguish active enhancers from promoters with high accuracy
983 (AUPR = 0.89, AUROC = 0.87). We were also able to identify
984 the most important features that distinguish promoters from
985 enhancers. In addition to TATA-box associated factors such as
986 TAF1, TAF7, and TBP, the RNA polymerase-II binding patterns
987 as well as chromatin remodelers such as KDM4A and PHF8 are
988 some of the most important factors that distinguish promoters
989 from enhancers in H1-hESC. This provides a framework that can
990 be utilized to identify the most important TFs associated with
991 active enhancers and promoters in each cell-type.

992 In Figure 6A, we show that the pattern of TF binding at
993 promoters is different from that at enhancers and TF-binding
994 at enhancers displaying more heterogeneity. As the set of TFs
995 binding promoters is fairly uniform, the same pairs of TF also
996 tend to bind together on promoters. In contrast, for enhancers,
997 the patterns of TF co-binding is much more heterogeneous and
998 different enhancers tend to contain different TF-pairs. This can
999 be observed in the patterns of TF co-binding in Figures 6C and
1000 S21. These TF co-associations could lead to mechanistic insights
1001 of cooperativity between TFs. For example, similar to a previous
1002 study [57], CTCF and ZNF143 may function cooperatively as they
1003 are observed to co-occur frequently at distal regulatory regions in
1004 this study.

1006 **Discussion**

1007 Our ability to accurately predict active enhancers in a cell-type
1008 specific manner using transferable supervised machine learning
1009 models that were trained based on regulatory regions identified
1010 using new NGS-enabled MPRAs distinguishes our method from
1011 previous enhancer prediction methods. Currently, most existing
1012 methods were parameterized (not properly “trained”) with re-
1013 gions that had various features associated with promoters and
1014 enhancers and only a small number of these regions were typically
1015 tested for regulatory activity experimentally in an *ad hoc* manner.
1016 The MPRAs were able to firmly establish that certain histone
1017 modifications occur on nucleosomes flanking active regulatory re-
1018 gions leading to the formation characteristic double peak pattern
1019 within the ChIP-signal [39]. This motivated us to create matched

1020 filter models that were able to identify these patterns within the
1021 shape of the ChIP-signal in the presence of stochastic noise with
1022 the highest signal to noise ratio. Furthermore, we were able to
1023 combine the matched filter scores from different epigenetic fea-
1024 tures using simple transferrable linear SVM models and learned
1025 the most informative epigenetic features for regulatory region
1026 predictions.

1027 The sensitivity and selectivity of various MPRAs is currently a
1028 matter of debate. A majority of these MPRAs test the regulatory
1029 activity of different regions by assessing their ability to induce
1030 gene expression in a plasmid after transfecting it into a cell-
1031 type of interest [31]. Such assays may not recapitulate the native
1032 chromatin environment found in chromosomes, which may be
1033 necessary for assessing whether the regulatory region is active in
1034 its genomic environment.

1035 Here, we show for the first time, that the patterns in the
1036 epigenetic signals associated with active enhancers identified
1037 using a transfection-based assay (STARR-seq) can be utilized
1038 to predict the activity of enhancers in a transduction-based
1039 assay (FIREWACH). During the FIREWACH assay, random
1040 nucleosome-free regions in mESC were captured and assayed
1041 for regulatory activity of the GFP gene by utilizing a lentiviral
1042 plasmid vector and inserted (or transduced) these vectors into
1043 the chromosome in mESC cells. As the FIREWACH assay tests
1044 the regulatory activity of enhancers after transduction, we assume
1045 that these regions were tested in their native chromatin environ-
1046 ment and transduction-based assays form a more stringent test
1047 for regulatory activity. However, due to the shorter length of the
1048 tested region (< 300 bp) and the single core promoter used in
1049 the FIREWACH assay, we think that the accuracy of the statistical
1050 models in Figure 4 is underestimated.

1051 We were able to assess the accuracy of different epigenetic
1052 metaprofiles for predicting regulatory activity using our statisti-
1053 cal models. While different acetylation modifications are as-
1054 sociated with active regions of the genome, we were able to
1055 compare close to 30 histone marks for enhancer and promoter
1056 predictions. The H3K27ac matched filter remains the single most
1057 important feature for predicting active regulatory regions while
1058 H3K4me1 and H3K4me3 are known to distinguish promoters
1059 from enhancers. However, our analysis characterizes the amount
1060 of redundancy in information within the metaprofile of differ-
1061 ent epigenetic features for predicting active regulatory regions
1062 and shows that ChIP-experiments of H2BK5ac, H4ac, and H2A
1063 variants could also produce independent information that can
1064 improve the accuracy of promoter and enhancer predictions. In
1065 addition to these 30-feature models, we also provide a simple to
1066 use six-parameter SVM model for combining H3K27ac, H3K9ac,
1067 H3K4me1, H3K4me2, H3K4me3, and DHS to predict active
1068 promoters and enhancers in a cell-type specific manner. We also
1069 showed that the metaprofiles and the combination of epigenetic
1070 marks associated with active regulatory regions are highly con-
1071 served in evolution making these models highly transferable.
1072 These six histone marks have been measured for a number of
1073 different tissues and cell-types by the Roadmap Epigenomics
1074 Mapping Consortium [39], the ENCODE [53], and the mod-
1075 ENCODE Consortium [58]. The enhancers predicted using our
1076 machine learning models were experimentally validated in human
1077 cell lines.

1078 One aspect that is discussed less frequently is the effect of
1079 core promoter on enhancer and promoter prediction. MPRAs
1080 show that the regulatory activity of enhancers and promoters in
1081 a regulatory assay depends on the core promoter used during
1082 the experiment [51]. As the transcription factors that bind to
1083 each regulatory region are thought to play a key role in core-
1084 promoter specificity [47, 51], we suspect that machine learning
1085 models that contain sequence or motif-based features may be
1086 biased towards certain transcription factor binding sites when
1087
1088

1089 trained with regulatory regions identified using a single-core
1090 promoter. To avoid such biases, it would be more appropriate to
1091 train models with sequence-based features when the validation
1092 experiments are performed with multiple core promoters. In the
1093 absence of validation data with multiple core promoters, it may
1094 be more suitable to train models using epigenetic features as such
1095 models contain no sequence-based information. In comparing the
1096 predictions from such models with experiments using a single core
1097 promoter, some of the strongest predictions may be mislabeled
1098 as negatives even though they contain some regulatory activity
1099 leading to a lower accuracy estimate as shown in Figure 2.

1100 As the epigenetic profiles and statistical models learned in
1101 this study are transferable across different cell-lines and species,
1102 we are able to apply these models to predict active enhancers
1103 and promoters in different cell-types. We applied these models to
1104 predict enhancers and promoters in H1-hESC, a highly studied
1105

1106 1. Banerji, J., S. Rusconi, and W. Schaffner, *Expression of a beta-globin gene is enhanced by remote SV40 DNA sequences*. Cell, 1981. **27**(2 Pt 1): p. 299-308.
1107 2. Ong, C.T. and V.G. Corces, *Enhancer function: new insights into the regulation of tissue-specific gene expression*. Nat Rev Genet, 2011. **12**(4): p. 283-93.
1108 3. Woolfe, A., et al., *Highly conserved non-coding sequences are associated with vertebrate development*. PLoS Biol, 2005. **3**(1): p. e7.
1109 4. Spitz, F. and E.E. Furlong, *Transcription factors: from enhancer binding to developmental control*. Nat Rev Genet, 2012. **13**(9): p. 613-26.
1110 5. Cotney, J., et al., *The evolution of lineage-specific regulatory activities in the human embryonic limb*. Cell, 2013. **154**(1): p. 185-96.
1111 6. Degner, J.F., et al., *DNase I sensitivity QTLs are a major determinant of human expression variation*. Nature, 2012. **482**(7385): p. 390-4.
1112 7. Shibata, Y., et al., *Extensive evolutionary changes in regulatory element activity during human origins are associated with altered gene expression and positive selection*. PLoS Genet, 2012. **8**(6): p. e1002789.
1113 8. Villar, D., et al., *Enhancer evolution across 20 mammalian species*. Cell, 2015. **160**(3): p. 554-66.
1114 9. Xiao, S., et al., *Comparative epigenomic annotation of regulatory DNA*. Cell, 2012. **149**(6): p. 1381-92.
1115 10. Wray, G.A., *The evolutionary significance of cis-regulatory mutations*. Nat Rev Genet, 2007. **8**(3): p. 206-16.
1116 11. Corradin, O. and P.C. Scacheri, *Enhancer variants: evaluating functions in common disease*. Genome Med, 2014. **6**(10): p. 85.
1117 12. Gusev, A., et al., *Partitioning heritability of regulatory and cell-type-specific variants across 11 common diseases*. Am J Hum Genet, 2014. **95**(5): p. 535-52.
1118 13. Slattery, M., et al., *Absence of a simple code: how transcription factors read the genome*. Trends Biochem Sci, 2014. **39**(9): p. 381-99.
1119 14. Levo, M., et al., *Unraveling determinants of transcription factor binding outside the core binding site*. Genome Res, 2015. **25**(7): p. 1018-29.
1120 15. Pennacchio, L.A., et al., *Enhancers: five essential questions*. Nat Rev Genet, 2013. **14**(4): p. 288-95.
1121 16. Erwin, G.D., et al., *Integrating diverse datasets improves developmental enhancer prediction*. PLoS Comput Biol, 2014. **10**(6): p. e1003677.
1122 17. Pennacchio, L.A., et al., *In vivo enhancer analysis of human conserved non-coding sequences*. Nature, 2006. **444**(7118): p. 499-502.
1123 18. Nord, A.S., et al., *Rapid and pervasive changes in genome-wide enhancer usage during mammalian development*. Cell, 2013. **155**(7): p. 1521-31.
1124 19. Visel, A., et al., *ChIP-seq accurately predicts tissue-specific activity of enhancers*. Nature, 2009. **457**(7231): p. 854-8.
1125 20. Andersson, R., et al., *An atlas of active enhancers across human cell types and tissues*. Nature, 2014. **507**(7493): p. 455-61.
1126 21. Narlikar, L., et al., *Genome-wide discovery of human heart enhancers*. Genome Res, 2010. **20**(3): p. 381-92.
1127 22. Visel, A., et al., *Ultraconservation identifies a small subset of extremely constrained developmental enhancers*. Nat Genet, 2008. **40**(2): p. 158-60.
1128 23. Bonn, S., et al., *Tissue-specific analysis of chromatin state identifies temporal signatures of enhancer activity during embryonic development*. Nat Genet, 2012. **44**(2): p. 148-56.
1129 24. Yip, K.Y., et al., *Classification of human genomic regions based on experimentally determined binding sites of more than 100 transcription-related factors*. Genome Biol, 2012. **13**(9): p. R48.
1130 25. Ghandi, M., et al., *Enhanced regulatory sequence prediction using gapped k-mer features*. PLoS Comput Biol, 2014. **10**(7): p. e1003711.
1131 26. Heintzman, N.D., et al., *Distinct and predictive chromatin signatures of transcriptional promoters and enhancers in the human genome*. Nat Genet, 2007. **39**(3): p. 311-8.
1132 27. Hoffman, M.M., et al., *Unsupervised pattern discovery in human chromatin structure through genomic segmentation*. Nat Methods, 2012. **9**(5): p. 473-6.
1133 28. Kharchenko, P.V., et al., *Comprehensive analysis of the chromatin landscape in Drosophila melanogaster*. Nature, 2011. **471**(7339): p. 480-5.
1134 29. He, H.H., et al., *Nucleosome dynamics define transcriptional enhancers*. Nat Genet, 2010. **42**(4): p. 343-7.

1135 ENCODE cell-line. This allowed us to analyze the differences
1136 in the patterns of TF binding at proximal and distal regulatory
1137 regions. The TF binding and co-binding patterns at enhancers
1138 is much more heterogeneous than that at promoters. We think
1139 that this heterogeneity in TF binding patterns makes it much
1140 more difficult to predict enhancers due to the absence of obvious
1141 sequence patterns in distal regulatory regions. However, we were
1142 also able to create highly accurate machine learning models that
1143 are able to distinguish proximal promoter regions from distal
1144 enhancers based on the patterns of TF ChIP-seq peaks within
1145 these regulatory regions. The conservation of the epigenetic underpinnings underlying active regulatory regions sets the stage for our method to study the evolution of tissue-specific enhancers and their genomic properties across different eukaryotic species.

1146 /body

1147 30. Ernst, J., et al., *Mapping and analysis of chromatin state dynamics in nine human cell types*. Nature, 2011. **473**(7345): p. 43-9.
1148 31. Arnold, C.D., et al., *Genome-wide quantitative enhancer activity maps identified by STARR-seq*. Science, 2013. **339**(6123): p. 1074-7.
1149 32. Dickel, D.E., et al., *Function-based identification of mammalian enhancers using site-specific integration*. Nat Methods, 2014. **11**(5): p. 566-71.
1150 33. Gisselbrecht, S.S., et al., *Highly parallel assays of tissue-specific enhancers in whole Drosophila embryos*. Nat Methods, 2013. **10**(8): p. 774-80.
1151 34. Kwasniewski, J.C., et al., *High-throughput functional testing of ENCODE segmentation predictions*. Genome Res, 2014. **24**(10): p. 1595-602.
1152 35. Melnikov, A., et al., *Systematic dissection and optimization of inducible enhancers in human cells using a massively parallel reporter assay*. Nat Biotechnol, 2012. **30**(3): p. 271-7.
1153 36. Murtha, M., et al., *FIREWACH: high-throughput functional detection of transcriptional regulatory modules in mammalian cells*. Nat Methods, 2014. **11**(5): p. 559-65.
1154 37. Patwardhan, R.P., et al., *Massively parallel functional dissection of mammalian enhancers in vivo*. Nat Biotechnol, 2012. **30**(3): p. 265-70.
1155 38. Yanez-Cuna, J.O., et al., *Dissection of thousands of cell type-specific enhancers identifies dinucleotide repeat motifs as general enhancer features*. Genome Res, 2014. **24**(7): p. 1147-56.
1156 39. Shlyueva, D., G. Stampfel, and A. Stark, *Transcriptional enhancers: from properties to genome-wide predictions*. Nat Rev Genet, 2014. **15**(4): p. 272-86.
1157 40. Maston, G.A., et al., *Characterization of enhancer function from genome-wide analyses*. Annu Rev Genomics Hum Genet, 2012. **13**: p. 29-57.
1158 41. Thurman, R.E., et al., *The accessible chromatin landscape of the human genome*. Nature, 2012. **489**(7414): p. 75-82.
1159 42. Kundaje, A., et al., *Ubiquitous heterogeneity and asymmetry of the chromatin environment at regulatory elements*. Genome Res, 2012. **22**(9): p. 1735-47.
1160 43. Kumar, V.B.V.K., A. Mahalanobis, and R.D. Juday, *Correlation Pattern Recognition*. 2005.
1161 44. Davis, J. and M. Goadrich, *The Relationship Between Precision-Recall and ROC Curves*. Proceedings of the 23rd international conference on Machine Learning, 2006: p. 233-240.
1162 45. Creyghton, M.P., et al., *Histone H3K27ac separates active from poised enhancers and predicts developmental state*. Proc Natl Acad Sci U S A, 2010. **107**(50): p. 21931-6.
1163 46. Rada-Iglesias, A., et al., *A unique chromatin signature uncovers early developmental enhancers in humans*. Nature, 2011. **470**(7333): p. 279-83.
1164 47. Butler, J.E. and J.T. Kadonaga, *Enhancer-promoter specificity mediated by DPE or TATA core promoter motifs*. Genes Dev, 2001. **15**(19): p. 2515-9.
1165 48. Li, X. and M. Noll, *Compatibility between enhancers and promoters determines the transcriptional specificity of gooseberry and gooseberry neuro in the Drosophila embryo*. EMBO J, 1994. **13**(2): p. 400-6.
1166 49. Merli, C., et al., *Promoter specificity mediates the independent regulation of neighboring genes*. Genes Dev, 1996. **10**(10): p. 1260-70.
1167 50. Ohtsuki, S., M. Levine, and H.N. Cai, *Different core promoters possess distinct regulatory activities in the Drosophila embryo*. Genes Dev, 1998. **12**(4): p. 547-56.
1168 51. Zabidi, M.A., et al., *Enhancer-core-promoter specificity separates developmental and house-keeping gene regulation*. Nature, 2015. **518**(7540): p. 556-9.
1169 52. Roadmap Epigenomics, C., et al., *Integrative analysis of 111 reference human epigenomes*. Nature, 2015. **518**(7539): p. 317-30.
1170 53. Consortium, E.P., *An integrated encyclopedia of DNA elements in the human genome*. Nature, 2012. **489**(7414): p. 57-74.
1171 54. Burges, C.J.C., *A Tutorial on Support Vector Machines for Pattern Recognition*. Data Mining and Knowledge Discovery, 1998. **2**: p. 121-167.
1172 55. Rajagopal, N., et al., *RFECS: a random-forest based algorithm for enhancer identification from chromatin state*. PLoS Comput Biol, 2013. **9**(3): p. e1002968.
1173 56. Koch, C.M., et al., *The landscape of histone modifications across 1% of the human genome in five human cell lines*. Genome Res, 2007. **17**(6): p. 691-707.
1174 57. Bailey, S.D., et al., *ZNF143 provides sequence specificity to secure chromatin interactions at gene promoters*. Nat Commun, 2015. **2**: p. 6186.
1175 58. mod, E.C., et al., *Identification of functional elements and regulatory circuits by Drosophila modENCODE*. Science, 2010. **330**(6012): p. 1787-97.

Please review all the figures in this paginated PDF and check if the figure size is appropriate to allow reading of the text in the figure.

If readability needs to be improved then resize the figure again in 'Figure sizing' interface of Article Sizing Tool.